# Electronic supplementary information

## Bridging the structural gap of supported vanadium oxides for oxidative dehydrogenation of propane with carbon dioxide

Li Wang[a, b], Heng-Bo Zhang[a], Rong-Rong Hu[a], Han-Qing Ge[a], Yong-Hong Song[a], Guo-Qing Yang[a,*], Yuefeng Li[b], Zhao-Tie Liu[a], Zhong-Wen Liu[a,*]

[a] Key Laboratory of Syngas Conversion of Shaanxi Province, School of Chemistry & Chemical Engineering, Shaanxi Normal University, Xi'an 710119, China

[b] Kaili Catalyst & New Materials Co., Ltd., Xi'an 710201, China

*: Corresponding author (G.-Q. Yang; Z.-W. Liu)

No. 620, West Chang'an Avenue

School of Chemistry & Chemical Engineering

Shaanxi Normal University

Xi'an 710119, China

E-mail: gqyang@snnu.edu.cn (G.-Q. Yang); zwliu@snnu.edu.cn (Z.-W. Liu)

## Table of Contents

## 1. Carbon balances of $CO_2$-ODP

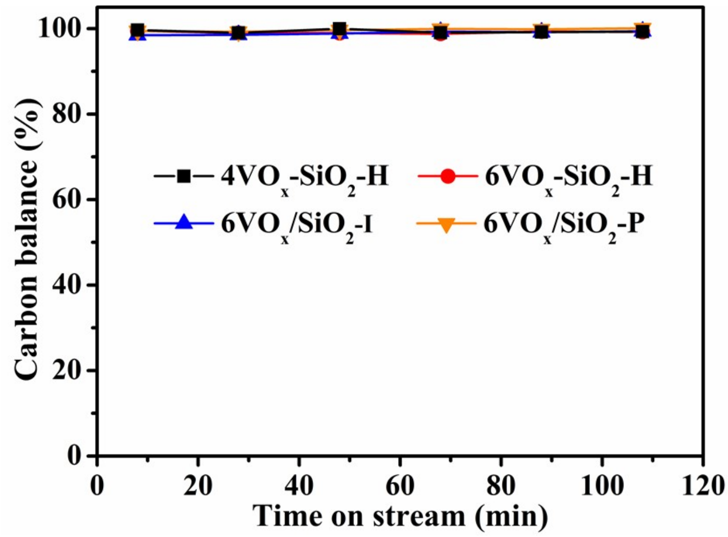


**Fig. S1** Carbon balances of $CO_2$-ODP over the catalysts with increasing TOS (The reaction conditions are the same as those given in Fig. 2).

## 2. $N_2$ adsorption/desorption isotherms of different catalysts

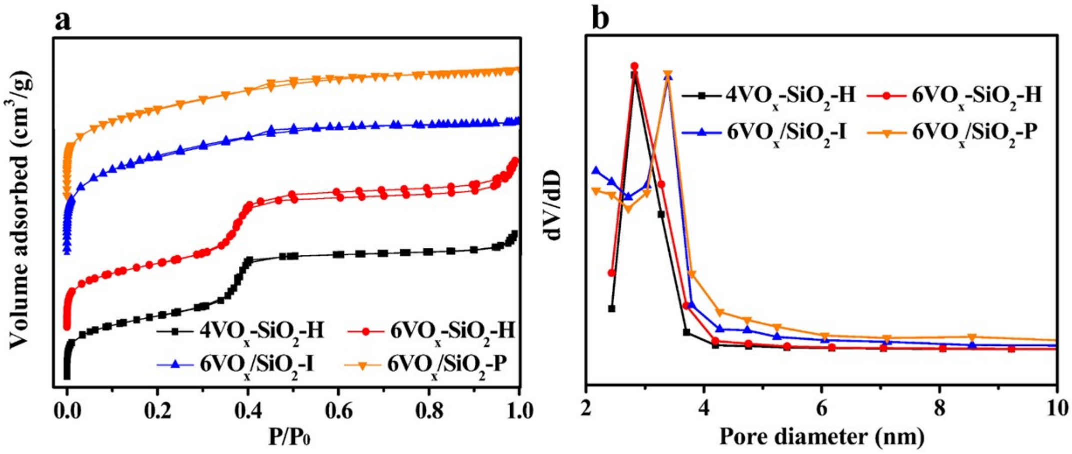


**Fig. S2** $N_2$ adsorption/desorption isotherms (a) and pore size distributions determined by the BJH method (b) for the catalysts.

.

### 3. Calculations of the adsorption edge energy from UV-vis DRS

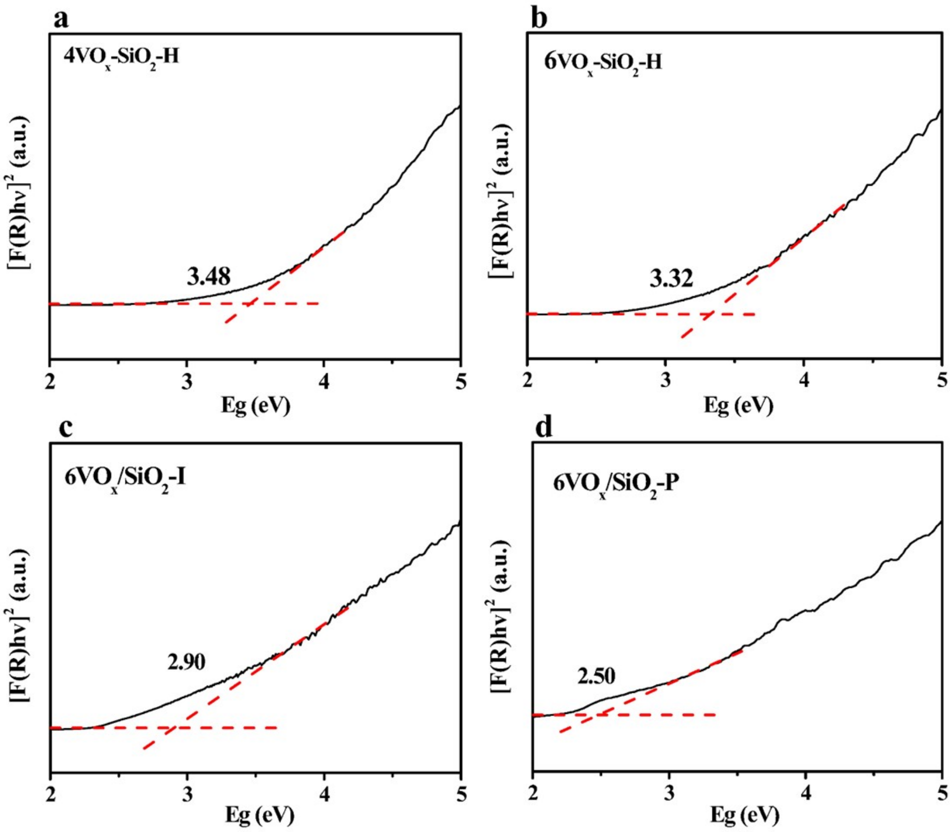


**Fig. S3** Absorption edge energy determined via UV-vis DRS of the catalysts.

## 4. V 2p XP spectra of fresh catalyst

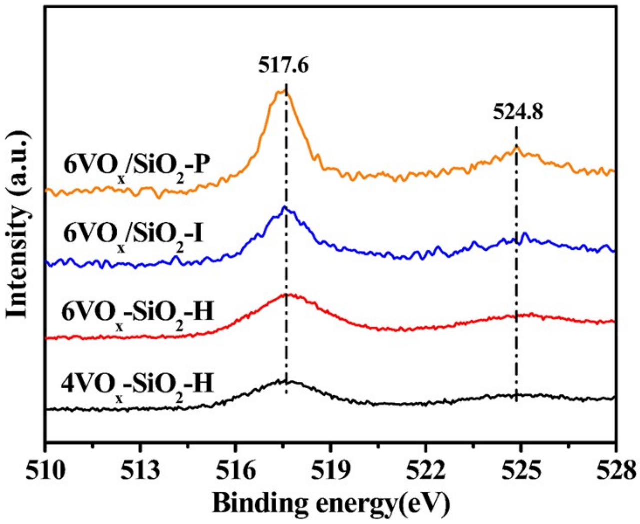


**Fig. S4** V 2p XP spectra of the fresh catalysts.

## 5. Time-on-stream catalytic results

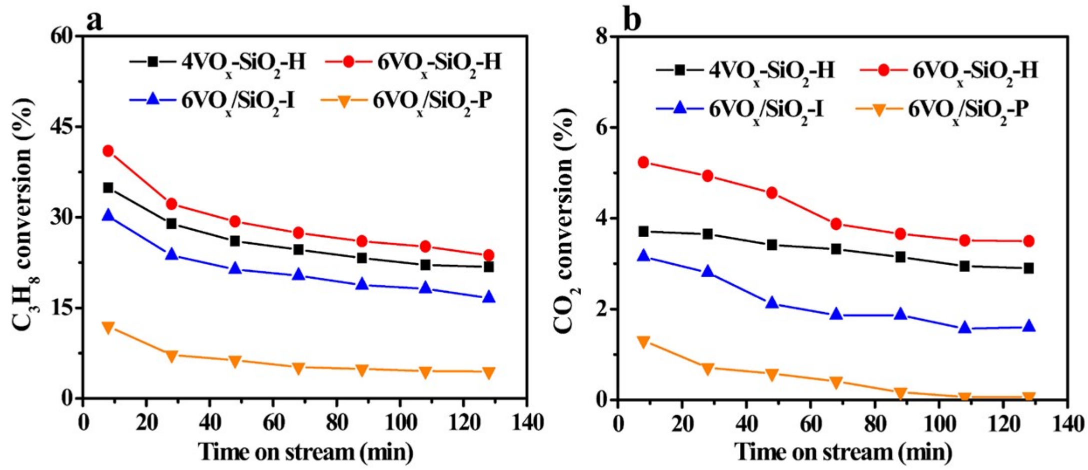


**Fig. S5** Time-on-stream conversions of $C_3H_8$ (a) and $CO_2$ (b) catalyzed by $4VO_x$-$SiO_2$-H**,** $6VO_x$-$SiO_2$-H, $6VO_x/SiO_2$-I and $6VO_x/SiO_2$-P (The reaction conditions are the same as those given in Fig. 2).

## 6. Relative deactivation rate of the catalysts

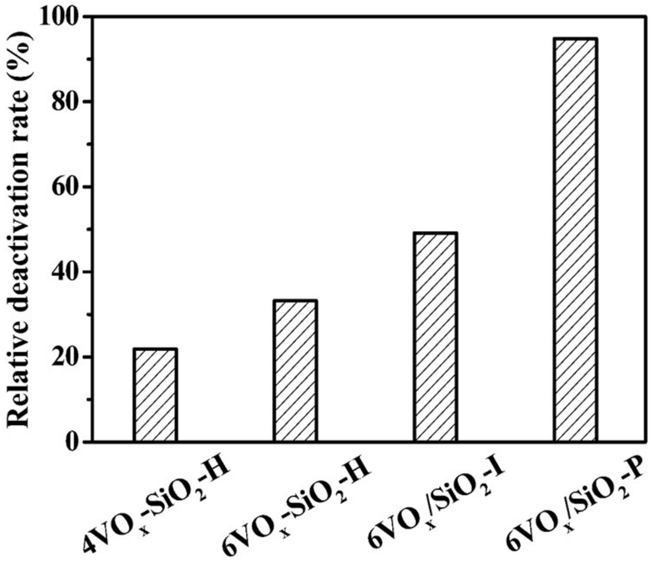


**Fig. S6** Relative deactivation rate of the catalysts calculated based on $CO_2$ conversion ($R_{CO2}$) for $CO_2$-ODP (The reaction conditions are the same as those given in Fig. 2).

## 7. Relationship between TOF($CO_2$) and Eg over the catalysts

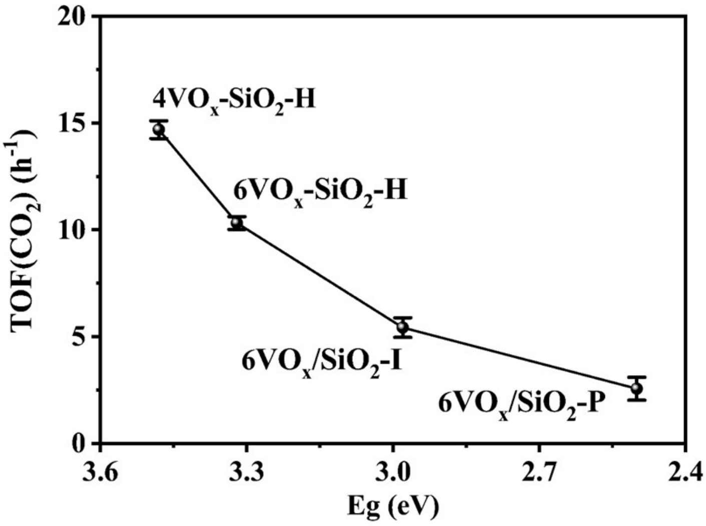


**Fig. S7** Relationship between TOF($CO_2$) and Eg derived from UV-vis DRS of the catalysts.

## 8. $CO_2$ pulse experiment for the $SiO_2$ support

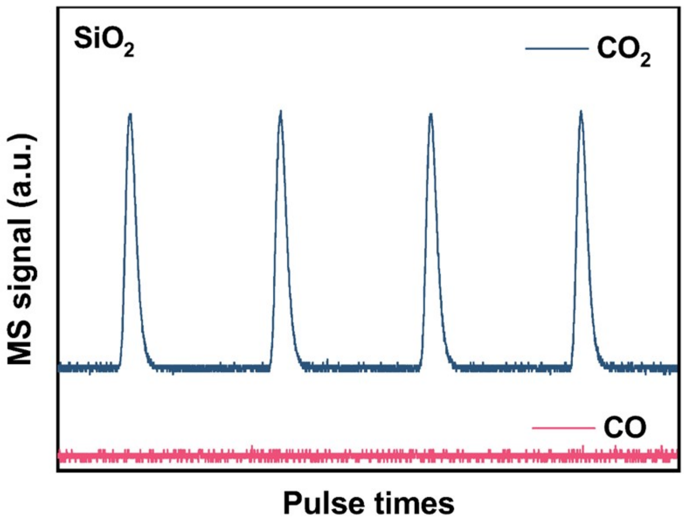


**Fig. S8** Transient MS response of the consecutive $CO_2$ pulses over the inert $SiO_2$ at 600 ºC.

## 9. TG results of spent catalysts

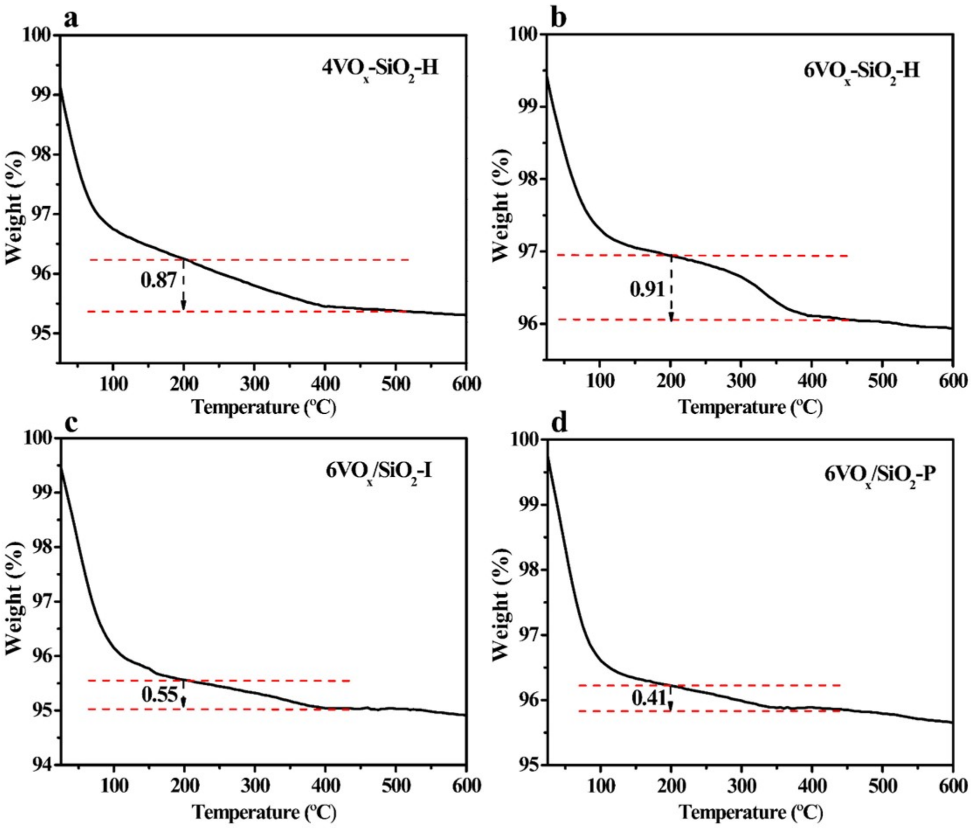


**Fig. S9** TG patterns of the spent catalysts for $CO_2$-ODP after a TOS of 128 min (The reaction conditions are the same as those given in Fig. 2, and the weight loss at 200-450 ºC is assigned to the burning of deposited coke species).

## 10. Raman results of spent catalysts

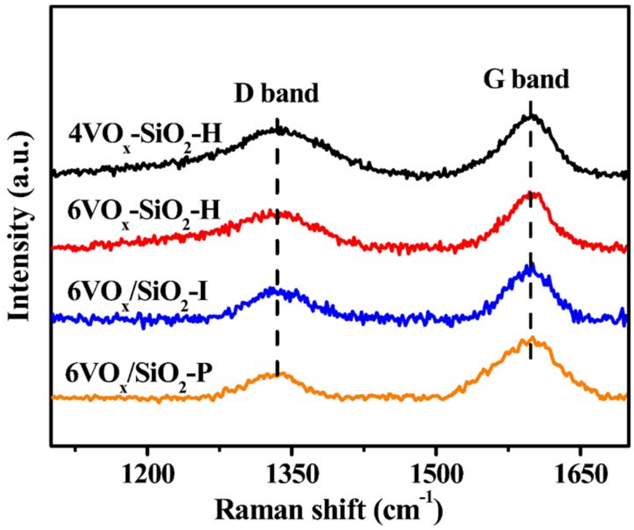


**Fig. S10** Visible Raman spectra of the spent catalyst for $CO_2$-ODP after a TOS of 128 min (The reaction conditions are the same as those given in Fig. 2).

## 11. Correlation of the relative deactivation rate with the V oxidation state of the spent catalysts

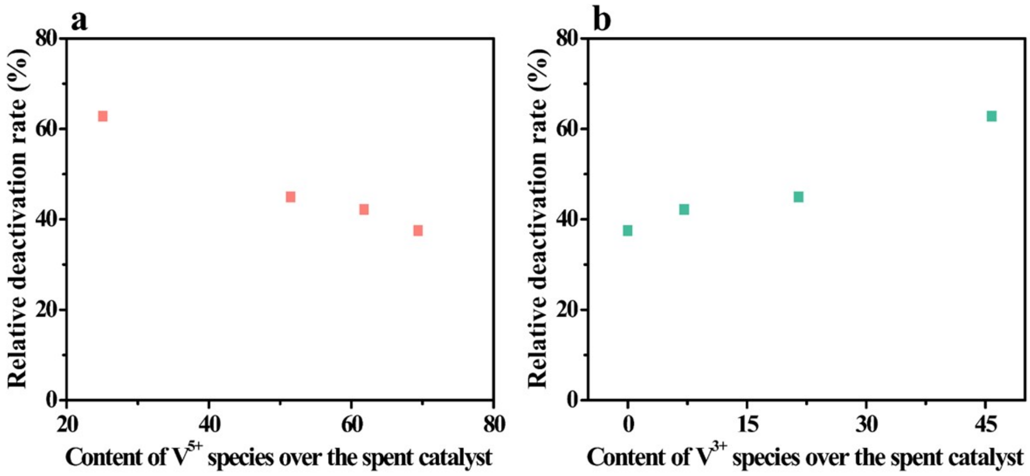


**Fig. S11** Correlation of the relative deactivation rate with the content of $V^{5+}$ and $V^{3+}$ species over the spent catalysts, respectively.

## 12. Estimation of the internal and external diffusion limitations

The internal and external diffusion limitations for $CO_2$-ODP are evaluated for the highest initial propane conversion of 41.0% at a TOS of 8 min over the $6VO_x$-$SiO_2$-H catalyst (Fig. 2a) under the reaction conditions of 600ºC, 0.1 MPa, $Ar/C_3H_8/CO_2$ molar ratio = 3/2/27, total flow rate = 32 mL/min, and GHSV = 7680 $mL\cdot g^{-1}\cdot h^{-1}$., and the catalyst particle size = 0.25-0.42 mm (40-60 mesh).

The potential mass transport limitations are estimated by using the Weisz-Prater criterion ($C_{WP}$) for the internal diffusion limitation (equation S1) and the Mears' criterion ($C_{MM}$) for the external diffusion resistance (equation S2). According to references, the effect of the internal and external diffusions on the catalytic reaction is negligible if

$$C_{WP} = \frac{-r_{obs}\rho_c R_p^2}{D_e C_s} < 1 \qquad \text{S1}$$

$$C_{MM} = \frac{-r_{obs}\rho_b R_p n}{k_c C_{Ab}} < 0.15 \qquad \text{S2}$$

Where $r_{obs}$ is observed reaction rate ($mol/kg_{cat}/s$); $\rho_c$ is density of solid catalyst ($kg/m^3$); $R_p$ is catalyst particle radius (m); $D_e$ is effective gas-phase diffusivity ($m^2/s$); $C_s$ is gas concentration of A at the external surface of the catalyst ($mol/m^3$); $\rho_b$ is bulk density of catalyst bed ($kg/m^3$) = $(1-\Phi)\rho_c$ ($\Phi$ = porosity); n is reaction order; $k_c$ is external mass transfer coefficient (m/s); $C_{Ab}$ is bulk gas concentration of A ($mol/m^3$).

The $D_e$ is calculated by the empirical formula (equation S3). The $D_{C_3H_8-CO_2}$ (binary gas-phase diffusivity) containing in equation S3 is calculated by the Chapman-Enskog empirical formula (equation S4). The collision integral $\Omega_{C_3H_8-CO_2}$ containing in equation S4 was calculated from the equation S5, which is the functional relationship of collision integral $\Omega_{C_3H_8-CO_2}$ and $k_BT/\varepsilon_{CO-H_2}$, where $k_B$ is Boltzmann constant and T is reaction temperature. The physical parameters $\sigma$ and $\varepsilon$ containing in equations S4 and S5 derived from the Lennard-Jones potential energy function, are determined by the equations S6 and S7, respectively, where $\sigma_{C_3H_8}$ = 5.118 Å,

$\sigma_{CO_2}$ = 3.941 Å, $\varepsilon / k_{B(C_3H_8)}$ = 237.1 $K^{-1}$, $\varepsilon / k_{B(CO_2)}$ = 195.2 $K^{-1}$. The $D_{Ki}$ (Knudsen diffusivity) is calculated by the empirical formula (equation S8), where $M_i$ and a are molar mass of reaction gas i, and the average pore radius of the catalyst determined from the $N_2$ adsorption-desorption isotherms (Fig. S2b), respectively.

$$D_e = \frac{1}{1/D_{C_3H_8-CO_2} + 1/D} \qquad S3$$

$$D_{C_3H_8-CO_2} = 0.001858T^{\frac{3}{2}} \frac{(\frac{1}{M_{C_3H_8}} + \frac{}{M}}{P\sigma^2_{C_3H_8-CO_2}\Omega_C} \qquad S4$$

$$\Omega_{C_3H_8-CO_2} = \frac{1}{(T/\varepsilon_{C_3H_8-CO_2})^{0.145}} + \frac{1}{(T/\varepsilon_{C_3H_8-CO_2}} \qquad S5$$

$$\sigma_{C_3H_8-CO_2} = \frac{1}{2}(\sigma_{C_3H_8} + \sigma_{CO_2}) = 4. \qquad S6$$

$$\varepsilon_{C_3H_8-CO_2} = (\varepsilon_{C_3H_8}\varepsilon_{CO_2})^{\frac{1}{2}} = 21 \qquad S7$$

$$D_{Ki} = 9700a(T/M_i)^{\frac{1}{2}} \qquad S8$$

The external mass transfer coefficient ($k_c$, m/s) of binary reaction gases from the bulk flow to the catalyst surface is calculated according to equation S9, which is derived from the mass-transfer correlation given in equation S10.

$$k_c = \frac{A\, D_{C_3H_8-CO_2}(\frac{\rho_g U d_p}{\mu\Phi})^{1/2}(\frac{\mu}{\rho_g D_{C_3H_8-C}}}{d_p} \qquad S9$$

$$Sh = A\,(Re^{1/2})(Sc^{1/3}),\ Sh = \frac{k_c d_p}{D_{C_3H_8-CO_2}},\ Re = \frac{\rho_g U d_p}{\mu\Phi},\ Sc = \frac{}{\rho_g D} \qquad S10$$

where A is a dimensionless constant of 2.6 with the assumption of homogeneous spherical catalyst particles at 40-60 mesh, U is the superficial velocity (m/s), μ is the dynamic viscosity (kg/m/s) of binary reaction gases, $d_p$ is the average diameter of the catalyst particle (m), and $\rho_g$ is the density of the binary reaction gases (kg/m$^3$). The values for the parameters are determined and given in Table S1.

**Table S1** The interpretation, unit and calculated result of the parameters relating to Weisz-Prater and Mears' criterion equations.

| Symbol | Interpretation | Unit | Value |
|---|---|---|---|
| $r_{obs}$ | Observed reaction rate | $mol \cdot kg_{cat}^{-1} \cdot s^{-1}$ | $3.67 \times 10^{-3}$ |
| n | Reaction order | -- | 1 |
| $R_p$ | Particle radius of the catalyst | m | $1.70 \times 10^{-4}$ |
| $\rho_c$ | Bulk density of the catalyst | $kg/m^3$ | 647.96 |
| $\rho_b$ | Bulk density of the catalyst bed | $kg/m^3$ | 473.92 |
| Φ | Porosity | % | 0.54 |
| a | Average pore radius of the catalyst | m | $3.70 \times 10^{-9}$ |
| $D_e$ | Effective diffusivity | $m^2 \cdot s^{-1}$ | $8.13 \times 10^{-6}$ |
| $C_s$ | Gas concentration of A at the external surface of the catalyst | $mol \cdot m^{-3}$ | 54.82 |
| $C_{Ab}$ | Bulk gas concentration of A | $mol \cdot m^{-3}$ | 54.82 |
| $k_c$ | External mass transfer coefficient | $m \cdot s^{-1}$ | $1.91 \times 10^{-3}$ |
| A | A dimensionless constant | -- | 2.60 |
| U | Superficial velocity | $m \cdot s^{-1}$ | 0.25 |
| μ | Dynamic viscosity | $kg \cdot m^{-1} \cdot s^{-1}$ | $3.13 \times 10^{-5}$ |
| $d_p$ | Average diameter of the catalyst particle | m | $3.40 \times 10^{-4}$ |
| $\rho_g$ | Density of the reaction gas | $kg \cdot m^{-3}$ | 0.83 |
| $D_{C_3H_8-CO_2}$ | Binary gas-phase diffusivity | $m^2 \cdot s^{-1}$ | $8.11 \times 10^{-6}$ |
| $D_{ki}$ | Knudsen diffusivity | $m^2 \cdot s^{-1}$ | $1.60 \times 10^{-4}$ |

The substitution of the values for the parameters into the $C_{WP}$ and $C_{MM}$ equations leads to

$$C_{WP} = \frac{-r_{obs}\rho_c R_p^2}{D_e C_s}$$

$$= \frac{\left[\left(3.67\times10^{-3}\ \mathrm{mol}\cdot\mathrm{kg}_{cat}^{-1}\mathrm{s}^{-1}\right)\times\left(647.96\ \mathrm{kg}\cdot\mathrm{m}^{-3}\right)\times\left(1.70\times10^{-4}\ \mathrm{m}\right)^2\right]}{\left[\left(8.13\times10^{-6}\ \mathrm{m}^2\cdot\mathrm{s}^{-1}\right)\times\left(54.82\ \mathrm{mol}\cdot\mathrm{m}^{-3}\right)\right]}$$

$$= 1.54\times10^{-3} < 1$$

$$C_{MM} = \frac{-r_{obs}\rho_b R_p n}{k_c C_{Ab}}$$

$$= \left[\frac{\left(3.67\times10^{-3}\ \mathrm{mol}\cdot\mathrm{kg}_{cat}^{-1}\cdot\mathrm{s}^{-1}\right)\times\left(473.92\ \mathrm{kg}\cdot\mathrm{m}^{-3}\right)\times\left(1.70\times10^{-4}\ \mathrm{m}\right)\times1}{\left(1.91\times10^{-3}\ \mathrm{m}\cdot\mathrm{s}^{-1}\right)\times\left(54.82\ \mathrm{mol}\cdot\mathrm{m}^{-3}\right)}\right]$$

$$= 2.82\times10^{-3} < 0.15$$

Thus, the internal and external diffusion limitations are negligible over the $VO_x$-$SiO_2$ catalysts for $CO_2$-ODP.